Dielectric properties of phase separated polymer solids: 1. Styrene–butadiene–styrene triblock copolymers

Alastair M. North, Richard A. Pethrick and Alexander D. Wilson*

Department of Pure and Applied Chemistry, University of Strathclyde, 295 Cathedral Street, Glasgow G1 1XL, UK

(Received 14 June 1977; revised 9 February 1978)

Theories currently applicable to the description of the low frequency dielectric loss, associated with trapping of charge carriers at interphase boundaries in polymers, are presented. Experimental observations on styrene–butadiene–styrene triblock copolymers are compared with theory. The interfacial polarization process in a film-cast copolymer with 30 wt % styrene was found to be in reasonable agreement with predictions for a morphology of parallel cylinders oriented at random, whereas that for a 50 wt % styrene copolymer was compatible with prediction for a random arrangement of partly parallel lamellae. These structures correspond to morphologies observed by electron microscopic observation. No evidence was found for a dielectric effect specifically requiring a diffuse conducting interfacial zone between the polystyrene and polybutadiene domains. The bulk d.c. conductivity also correlated with predictions made using the same parameters as those involved in calculation of the relaxation effects.

INTRODUCTION

Phase separation, well-established as a dominant feature in determining the properties of block copolymers, also occurs in partly crystalline homopolymers[1–6]. The direct observation of polymer morphology by electron microscopy provides a simple means of correlating phase structure and macroscopic dynamic properties. In mechanical observations, phase separation causes distinct changes in both the dynamic and ultimate strength of the material[1,2]. Similarly diffusivity[3–5] and dielectric behaviour[5,6] show significant changes on phase separation. In particular, if the constituent phases possess markedly different electrical conductivities, trapping of charge carriers at phase boundaries leads to low frequency dielectric dispersion phenomena[7,8]. The position, shape and amplitude of this dispersion is dependent on the anisotropy, orientation and electrical properties of each phase.

A variety of theories have been proposed to describe this type of phenomenon[7–28]. In practice, apart from a very few rather specialized and somewhat artificial situations[9,10], quantitative comparison of theory and experiment has not been very successful, particularly for polymers[24]. One reason for this failure has been an inability to describe accurately the complex morphologies found in most polymers.

In this paper useful theories available for the description of the dielectric properties of phase separated polymers are reviewed. A study of the dielectric properties of a system with a simplified, well-characterized morphology, styrene–butadiene–styrene triblock copolymer, is reported and discussed in the context of these theories.

* Present address: Proctor and Gamble Ltd, Newcastle Technical Centre (2), Whitley Road, Longbenton, Newcastle-upon-Tyne NE12 9TS, UK.

0032–3861/78/1908–0913$03.00

Dielectric properties of heterogeneous systems

Permittivity increment. The simplest models[7,9,10] of a heterogeneous dielectric consider the solid as an ensemble of isotropic ellipsoids of permittivity ϵ_2 and volume fraction v_2 embedded in a matrix of permittivity ϵ_1, both phases having zero conductivity and $\epsilon_2 > \epsilon_1$. The orientation of the ellipsoid axes (a, b, c) relative to the applied electric field can be defined by the angles γ_i $(i = a, b, c)$. The permittivity of this simple solid is described by the Maxwell–Wagner–Sillars model (MWS):

$$\epsilon = \epsilon_1 \left[1 + v_2(\epsilon_2 - \epsilon_1) \sum_i \frac{\cos^2\gamma_i}{\epsilon_1 + A_i(1 - v_2)(\epsilon_2 - \epsilon_1)} \right] \quad (1)$$

where A_i is the depolarization ratio of the constituent ellipsoids along the i-axis and is defined by:

$$A_a = \frac{abc}{2} \int_0^\infty \frac{\partial s}{(s + a^2)[(s + a^2)(s + b^2)(s + c^2)]^{1/2}} \quad (2)$$

where s is the positive root of the equation of the confocal ellipsoid $[x^2/(a^2 + u) + y^2/(b^2 + u) + z^2/(c^2 + u)] = 1$, where u is a point outside the ellipsoid $(x^2/a^2) + (y^2/b^2) + (z^2/c^2) = 1$.

The coefficient A_a has a value of unity for lamellae, equals 1/3 for spheres and tends to zero for long thin rods. The only orientations which lead to simple analytical forms of equation (1) are as follows:

(i) The a-axis oriented parallel to the electric field:

$$\cos^2\gamma_a = 1: \qquad \cos^2\gamma_b = \cos^2\gamma_c = 0.$$

(ii) The a-axis oriented perpendicular to the electric field:

$$\cos^2\gamma_a = \cos^2\gamma_b = 0: \qquad \cos^2\gamma_c = 1$$

(iii) A random orientation of ellipsoids:

$$\cos^2\gamma_a = \cos^2\gamma_b = \cos^2\gamma_c = 1/3.$$

In general, with the a-axis parallel to the electric field, an ensemble of rods gives a larger permittivity than a system of spheres or random ellipsoids, which in turn are higher than perpendicular ellipsoids or a perpendicular lamellar structure. Systems polydisperse in the size of the occluded domains can be described by equation (1) provided $v_2 < 0.2$. In fact equation (1) with $A_a = 1/3$ has been shown to be valid[10] only for samples in which there is a size gradation of the disperse phase.

At higher concentrations of the dispersed phase electrostatic interactions between domains become significant and modified expressions are required, *viz*:

(a) Bruggeman[12] equation:

$$\frac{\epsilon_2 - \epsilon}{\epsilon_2 - \epsilon_1}\left(\frac{\epsilon_1}{\epsilon}\right)^{1/3} = 1 - v_2 \tag{3}$$

(b) Looyenga[13] equation:

$$\frac{\epsilon^{1/3} - \epsilon_1^{1/3}}{\epsilon_2^{1/3} - \epsilon_1^{1/3}} = v_2 \tag{4}$$

Both relationships are applicable to concentrated dispersions of spheres, while Davies[14] has shown equation (4) to hold for morphologies in which distinction between disperse and matrix phases are lost, as when each phase forms semi-continuous paths.

Dielectric dispersion. The position in the frequency or time domain of the dielectric dispersion[7,9,10] and its shape, may be obtained by substituting the complex admittances $[\Delta_i = \sigma_i + j\omega\epsilon_i(j\omega)]$ for the ϵ_i in the permittivity equations appropriate to the morphology being studied. For dilute dispersions in which the conductivity of the occluded phase, σ_2, is greater than that of the matrix phase, σ_1, the relaxation equations obtained from equation (1) are:

$$\epsilon_0 = \epsilon_1\left[1 + v_2(\sigma_2 - \sigma_1)\sum \frac{\cos^2\gamma_i}{\sigma_1 + A_i(1 - v_2)(\sigma_2 - \sigma_1)}\right.$$

$$\left. + v_2\sigma_1 \sum \frac{\cos^2\gamma_i(\sigma_1\epsilon_2 - \sigma_2\epsilon_1)}{[\sigma_1 + A_i(1 - v_2)(\sigma_2 - \sigma_1)^2}\right] \tag{5}$$

$$\tau = \epsilon\left[\frac{\epsilon_1 + A_i(1 - v_2)(\epsilon_2 - \epsilon_1)}{\sigma_1 + A_i(1 - v_2)(\sigma_2 - \sigma_1)}\right] \tag{6}$$

where ϵ is the permittivity of free space.

For an axially isotropic dispersion of phases the Debye approximation of a single relaxation time, τ, may be used:

$$\frac{\epsilon' - \epsilon_\infty}{\epsilon_0 - \epsilon_\infty} = \frac{1}{1 + \omega^2\tau^2} \tag{7}$$

$$\frac{\epsilon''}{\epsilon_0 - \epsilon_\infty} = \frac{\omega\tau}{1 + \omega^2\tau^2} \tag{8}$$

Randomly oriented dispersed phases may be represented by an equal combination of three Debye processes[18]. The relaxation amplitude and time are both increased by ellipsoid elongation in the field direction, and this can lead to increases of several orders of magnitude.

Reversal of the relative magnitudes of the conductivities of the continuous and discontinuous phases ($\sigma_1 > \sigma_2$) leads to a reduction in the magnitude of the dielectric dispersion in all cases except the parallel lamellar morphology.

These simple models for low volume fractions of a second phase have been discussed extensively by Sillars[9], and the various relationships are summarized in *Table 1*.

In this review we are concerned principally with the case usually encountered in polymer solids of a high volume fraction of dispersed phase. As can be seen from *Table 1*, $\Delta\epsilon/v_2$ in such cases is larger than for dilute suspensions, although the relaxation time is unaffected[19–22].

Effect of space charge. In the simplest models (MWS) the interfacial polarization is assumed to arise from charges located on an infinitely thin layer surrounding the dispersed phase. In practice, the layer may have a finite thickness of the order of the Debye shielding radius χ^{-1} where[23]:

$$\chi^{-1} = \left(\frac{\epsilon\epsilon_2 kT}{2e^2 n}\right)^{1/2} \tag{9}$$

where ϵ is the permittivity of free space n is the charge carrier density, e is the charge on an electron and ϵ_2, k and T have their usual meaning.

This diffusion layer leads to a decrease (with increasing χ^{-1}) in both the magnitude of the dispersion and its relaxation time compared with the predictions of the simple theory both for spherical and lamellar morphologies[24]. The effect is significant when $\chi l\epsilon_1/\epsilon_2 \leqslant 10$ where l is the domain diameter or thickness. In addition a dependence is introduced into the relaxation behaviour.

Surface conductivity. A clear inadequacy of the simple theories is the assumption of sharp boundaries between the constituent phases. In reality, the occluded domain will be surrounded by a diffuse region with dielectric properties (ϵ_s, σ_s) different from either of the pure phases. Analysis of this type of model[25] predicts that two distinct dispersion regions should be observed. In the limit, when the boundary becomes very thin and is of extremely high conductivity, ($\sigma_s \gg \sigma_1, \sigma_2$), one dispersion region predominates and occurs at higher frequency with a larger amplitude than would be expected for a system without the conducting layer.

Two refinements of this model are worth mentioning. Both involve the surface conductivity, which in the first[26] is independent of frequency and in the second[27] exhibits a frequency dependence. In the first case[26] the surface conductivity is given by:

$$\lambda_s = \sum_i n_i\eta_i^s q_i \tag{10}$$

with an infinitely thin interfacial region, $\chi l > 1$, n_i is the charge carrier density at the surface, η_i^s is the mobility of

Table 1

(a) MWS relations for low volume fraction dispersions: $v_2 < 0.2$: $\chi l < 1$

Morphology	Reference	ϵ_∞ (equation 1): ϵ_0 (equation 5); τ (equation 6)
Spheres	Wagner[10]	$A_a = 1/3$: $\cos^2\gamma_a = 1$; $\cos^2\gamma_b = \cos^2\gamma_c = 0$
Ellipsoids (*a*-axis parallel)	Sillars (11)[9]	All A_a: $\cos^2\gamma_a = 1$; $\cos^2\gamma_b = \cos^2\gamma_c = 0$
Ellipsoids (*a*-axis perpendicular)	Sillars (1)[9]	$0 \leqslant A_b \leqslant 0.5$: $\cos^2\gamma_b = 1$; $\cos^2\gamma_a = \cos^2\gamma_c = 0$
Ellipsoids (random)	Fricke[18]	All A_i: $\cos^2\gamma_i = 1/3$

(b) MWS relations for concentrated dispersions: all v_2: $\chi l < 1$

Morphology	Reference	ϵ_∞	ϵ_0	τ
Spheres	Bruggemaan[12] Hanai[19,20]	Equation (3)	$\epsilon_0\left[\frac{3}{\sigma-\sigma_2}-\frac{1}{\sigma}\right] = 3\left[\frac{\epsilon_2-\epsilon_1}{\sigma_2-\sigma_1}+\frac{\epsilon_2}{\sigma-\sigma_2}\right]-\frac{\epsilon_2}{\sigma_1}$	Not given
(i) Spheres (ii) Semi-continuous network	Loeyenga[13]	Equation (4)	–	–

(c) Modification of MWS relations in presence of space charge layer: $v_2 < 0.05$: all χl. Reference: Truckan[23]

Morphology	ϵ_∞	ϵ_0	τ
Spheres (radius/2)	$\epsilon_\infty = \epsilon_1\left[1+3v_2\frac{\epsilon_2-\epsilon_2}{2\epsilon_1+\epsilon_2}\right]$	$\epsilon_0 = \epsilon_1\{1+3v_2 \times \frac{(\chi l)^2 th\left(\frac{\chi l}{2}\right)+\frac{2(2\epsilon_2+\epsilon_1)}{\epsilon_2}\left[2th\left(\frac{\chi l}{2}\right)-\chi l\right]}{(\chi l)^2 th\left(\frac{\chi l}{2}\right)+\frac{4(\epsilon_2-\epsilon_1)}{\epsilon_2}\left[2th\left(\frac{\chi l}{2}\right)-\chi l\right]}\}$	$\tau = \frac{\epsilon(2\epsilon_1+\epsilon_2)}{(2\sigma_1+\sigma_2)} \times \frac{(\chi l)^2 th\left(\frac{\chi l}{2}\right)+6\left[2th\left(\frac{\chi l}{2}\right)-\chi l\right]}{(\chi l)^2 th\left(\frac{\chi l}{2}\right)-\frac{4(\epsilon_1-\epsilon_2)}{\epsilon_2}\left[2th\left(\frac{\chi l}{2}\right)-\chi l\right]}$

(d) Relations for systems with surface conductivities

Morphology	Reference	ϵ_∞	ϵ_0	τ
Spheres (radius a)	O'Konski[26]	In the MWS relations of *Table 1a* σ_2 is replaced by $\sigma_2 + \lambda_s\, 2/a$		
Ellipsoids (*a*, *b* = *c*)	O'Konski[26]	In the MWS relations of *Table 1a* σ_2 is replaced by $\sigma_2 + K_i\lambda_s$ where $K_a = \sigma^2/b$ and $K_b = K_c = \sigma^4/\pi b$		
Spheres (radius a)	Schwarz[27]	Equation (1): $A_a = 1/3$; $\cos^2\gamma_a = 1$; $\cos^2\gamma_b = \cos^2\gamma_c = 0$	$\epsilon_\infty + \frac{9e^2\sigma' a v_1}{4\epsilon kT[1+(v_1/2)^2]}$	$\tau = a^2/(2\eta^s kT)$
Ellipsoids (*a*-axis parallal)	Takashima[28]	Equation (1): all A_i; $\cos^2\gamma_a = 1$; $\cos^2\gamma_b = \cos^2\gamma_c = 0$	$\epsilon_\infty + \frac{9e^2\sigma' a^2 v_1}{8\epsilon kTb(1+v_1)^2}$	$\tau = \frac{a^2+b^2}{2\eta^s kT}$
Ellipsoids (random)	Takashima[28]	Equation (1): all A_i; $\cos^2\gamma_a = 1/3$	$\epsilon_\infty + \frac{e^2\sigma' v_1}{3kT(1+V_1)^2\epsilon}\left[\frac{9}{8}\frac{a^2}{b}+2b\right]$	$\tau_a = \frac{a^2+b^2}{2\eta^s kT}$; τ_b Not given

* Trukhan[23] uses a simplified form of Wagner's theory[10] (v_2 very small, $\sigma_1 \ll \sigma_2$)

the charge q_i. The relaxation behaviour is obtained by replacing σ_2 in the simple model by $(\sigma_2 + k\lambda_s)$ where k is dependent on both the shape and size of the dispersed phase. For spheres of radius a, $k = 2/a$, while for long thin rods ($a \gg b = c$) $k_a = 2/b$ and $k_b = k_c = 4/\pi b$.

It has been pointed out that the conductivity may be frequency-dependent due to localization of charge by a strong electrostatic interaction with the surface of the dispersed phase. This theory predicts that the equilibrium polarization is governed by surface diffusion, and the relaxation time is directly related to the time required for the charge carrier to diffuse over a distance of the order of the particle diameter. A limitation of this approach is that it ignores the possibility of exchange between bound charge carriers and the bulk of the matrix phase. It has been argued[24] that since the applied field displaces the mobile ions, but not the fixed charge, there is a departure from equilibrium at the interface. As a result of the motion, electric fluxes are induced normal to the surface, and these give rise to an oscillating diffuse volume at the interface reducing the relaxation time and di-

Table 2 Characteristics of polymers studied

Polymer	Code	$M_W \times 10^5$	M_W/M_n	Composition of copolymer: 1,2-Butadiene (mol %)	Styrene (mol %)	Styrene (wt %)
Polybutadiene	PB	1.76	–	10	–	–
SBS (30 wt %)	30 SP	1.71	1.1	8	21.3	34 3
SBS (50 wt %)	50 SP	1.70	1.1	9	34.1	49.9
Polymers doped with benzoic acid:						
SBS (30 wt %)	30 SD 2.5	–	–	2.5 wt % Benzoic acid		
	30 SD 3.8	–	–	3.8 wt % Benzoic acid		
SBS (50 wt %)	50 SD 2.5	–	–	2.5 wt % Benzoic acid		

electric increment by $(1 + 2\chi n_s/n)$, where n_s is the charge carrier density in the interface and n is the bulk charge carrier density. Such analyses are included in *Table 1.*

Comparison of theory and experimental observation in polymer systems

Almost all polymer systems studied exhibit interfacial polarization with the following characteristics[29–35]. The loss is often of high magnitude ($\epsilon'' > 100$)[31,32] and has a temperature coefficient (activation energy) which mirrors that for d.c. conduction[20,30]. While the conductivity and relaxation frequency are increased by adsorbed moisture, the relaxation magnitude may be increased or decreased[8,29,33]. This seems to indicate that in these polymers, generally non-polar and non-conducting, the interfacial polarization involves the same charge carriers (perhaps arising from spurious ionic or ionizable impurities) as does d.c. conduction. There is a general lack of data relating the dielectric increment to the volume fraction of the dispersed phase. This reflects the lack of reproducibility of morphology in many samples, even when obtained from the same polymeric material[35].

A study of the relaxation magnitude in a series of nylons[30] indicated an increase with increasing crystallinity. However, the observed dielectric increment was much higher than predicted by simple MWS theory[29].

Better agreement would have been obtained if the dispersed phase had been assumed to be ellipsoidal, which is consistent with current theories of the morphology in these systems[36].

Measurements made on surfactant-doped polyethylene[37] in which the detergent forms a highly conducting layer at the crystallite interface gave reasonable agreement with theory Similar close correspondence between theory and experiment has been observed in poly(vinylidene fluoride)[38] where a diffuse double layer was considered to exist at crystallite surfaces. However, in virtually all the cases studied the simple MWS theory is inapplicable.

One of the difficulties in such work has been in obtaining samples with a simple clearly defined, two-phase geometry. For this reason the principal objective of this study was to ascertain the correlation between morphology and dielectric behaviour in materials of well characterized two-phase geometry.

Although interfacial polarization in non-polar or non-conducting materials occurs at low frequencies, it must be emphasized that other phenomena, too, can cause dielectric loss at similar frequencies. The blocking of charge carriers at sample–electrode interfaces[15,16], and charge carrier hopping between trapping sites are two such phenomena[7,9,10,17]. The former can usually be detected by varying sample and electrode geometries, while the latter is a general phenomenon of which interfacial 'trapping' can be considered a special case.

EXPERIMENTAL

Materials

Styrene–butadiene–styrene copolymers, Cariflex TR4113 and TR4122, were supplied by Shell Chemicals. Polybutadiene, Intene, was supplied by the International Synthetic Rubber Company.

All polymers were purified before use by reprecipitation from benzene using methanol. Molecular weights were obtained by gel permeation chromatography (g.p.c.) using a Waters Anaprep Al, (*Table 2*). The styrene and vinyl butadiene content were estimated from 220 MHz n.m.r. spectra (*Table 2*). Since the proton resonances of the *cis-* and *trans-*1,4-olefinic protons are separated by less than 0.05 ppm estimation of the *cis/trans* ratio was very approximate. However the resonances centred at 5.4 ppm were very similar for the three polymers, indicating a similar isomeric structure in each case. For n-butyllithium-initiated polybutadiene the expected microstructure is 50% *trans,* 40% *cis* and 10% vinyl and the reported p.m.r. spectra[59,60] are identical to those of the present polymer.

Sample preparation

Samples for dielectric measurement were obtained in the form of flat uniform discs, 50 mm in diameter and approximately 1 mm thick, by evaporation of dilute solutions, 0.5 wt %, on a flat 'Melinex' surface. In order to ensure that samples attained well-defined morphologies, evaporation was controlled to occur slowly over a period of about 10 days. Samples were heated under vacuum for 24 h at 390K to allow evaporation of residual solvent and annealing processes to take place. During this final stage aluminium foil electrodes were applied to the sample surfaces while heating under slight pressure above the sample softening point.

Electrical measurements

Dielectric measurements were performed over the frequency range 10^4 to 10^{-5} Hz using a combination of transformer ratio-arm bridge (10^4–10^2 Hz), Scheiber bridge[39] (10^2–10^{-1} Hz) and d.c. transient (10^{-1}–10^{-5} Hz) techniques[40]. Current–time data were converted to the appropriate permittivity–frequency representation using an integrated Fourier transformation[34,35,41], rather than the appropriate Hamon transform.

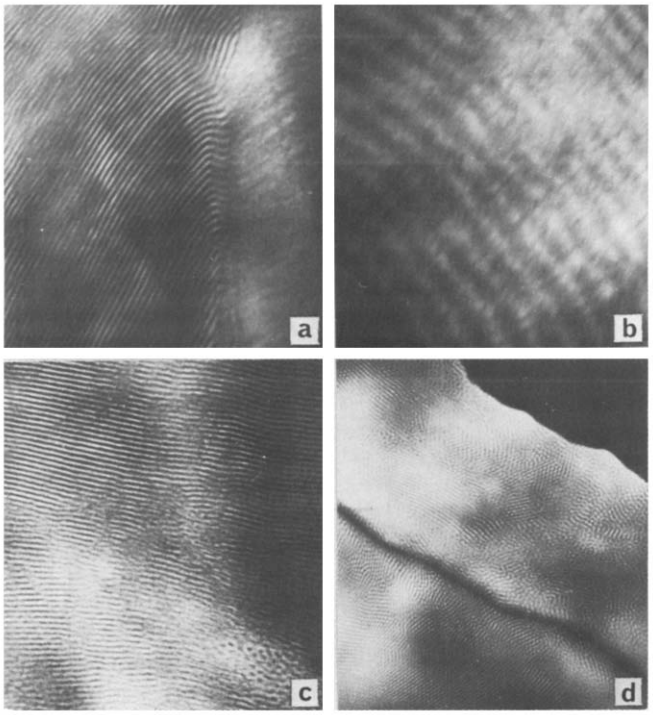

Figure 1 Transmission electron micrograph of styrene–butadiene–styrene copolymers. (a) 50 SP section; (b) 50 SP section; (c) 30 SP section; (d) 30 SP section

Electron microscopy

Thin sections for transmission electron microscopy were obtained by ultramicrotoming at 130K using 2-methyl pentane as the trough liquid. The sections were stained by exposure to a 0.1% aqueous solution of osmium tetroxide for 30 min. The polybutadiene phase as a consequence appears black in the micrographs[42]. The AE1 EM6G electron microscope used in this study had a resolution of better than 1 nm.

Differential scanning calorimetry

Glass transitions were measured using a Perkin–Elmer DSC–1. Studies on the benzoic acid-doped samples exhibited only one endotherm between 330 and 410K attributed to the T_g of the polystyrene domains. The absence of any additional features indicates that the benzoic acid is molecularly dispersed.

RESULTS AND DISCUSSION

Sample morphologies

The electron micrographs were obtained from specimens sectioned perpendicular to the film surface, and so illustrate representative average morphologies for the bulk of the sample.

The copolymer with 50 wt % of polystyrene shows alternating polybutadiene (PB) and polystyrene (PS) domains of 13 nm thickness. These extend over a distance greater than 1 μm, *Figure 1a*. Comparison of the known phase volume fractions with those calculated from the phase dimensions for several model morphologies, indicates that the sample consists of alternating lamellae of styrene and butadiene. The micrograph of another section, *Figure 1b*, showing larger domains, is consistent with a slanting section through a lamellar morphology.

Alternating regions were also observed in the copolymer with 30 wt % polystyrene (*Figure 1c*). However, comparison of the known and calculated phase volume fractions indicates that the preferred morphology should consist of rods of polystyrene in a butadiene matrix. This discrete rod morphology was in fact observed in certain sections (*Figure 1d*). The polystyrene rods were 20 nm in diameter with a 40 nm repeat distance.

The morphologies described above are in good agreement with those reported previously[43–45]. However some evidence of long range structural disorder, and regions of phase inversion or poorly defined phase separation, were observed in certain of the sections studied. Some of the ordered regions were interconnected to form extensive areas or 'grains'. These 'grains' were variously oriented to each other within the sample. No information on the sharpness of the interfacial region can be obtained from the electron micrographs. However it has been suggested on a theoretical basis[46] that in these polymers, up to 25% of the sample volume may be occupied by the interface. Nevertheless, the lamellar and cylindrical morphologies described above can be considered generally representative of the bulk of the polymer.

High frequency dielectric relaxation

Dielectric measurements of the high frequency relaxation in the SBS copolymers (*Figure 2*) are in good agreement with previously reported measurements. The dielectric loss peak is ascribed to micro-Brownian motion of the polybutadiene chain[47–49]. In the case of the copolymer with 30 wt % styrene, the loss peak is virtually identical (in position on the temperature axis) with that of polybutadiene. However, the copolymer with 50 wt % styrene exhibits a loss peak shifted to higher temperature. Similar results have been reported from related dynamic studies[47]. A plot of the position of ΔT_{max} against volume fraction of polystyrene, *Figure 3*, clearly indicates that a distinct transition occurs at V_{ps} between 0.4 and 0.7. This transition can be correlated with a corresponding variation in the shear modulus of the copolymer[49]. It has been attributed to a change of morphology from a polybutadiene continuous phase to one in which both polybutadiene and polystyrene exhibit phase continuity. In the region of lamellar morphology the polybutadiene volume is constrained by the lower thermal expansivity of the glassy polystyrene domains and so has a lower effective coefficient of expansion, α. The shift in T_{max} may be

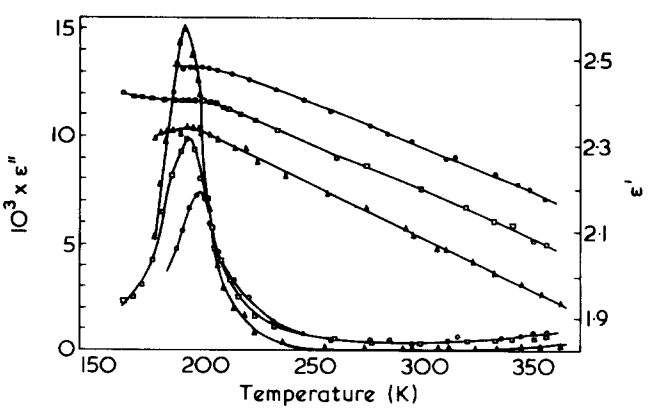

Figure 2 A.c. dielectric spectra at 1.34 kHz. △, PB; □, 30 SP; ○, 50 SP

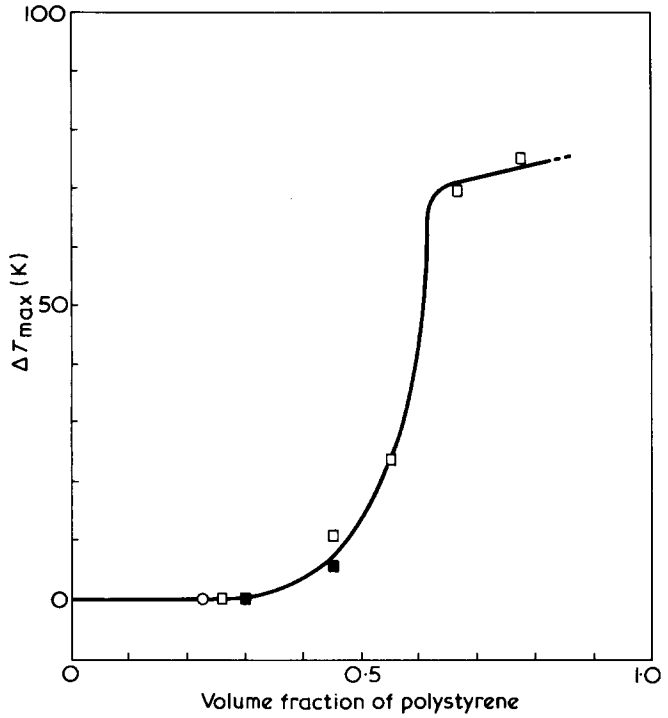

Figure 3 Dependence of ΔT_{max} (the difference between T_{max} copolymer and T_{max} polybutadiene) on the volume fraction of polystyrene in the copolymers. ○, Dielectric and acoustic data[47]; □, n.m.r. data[50]; ■, this work

Table 3 Relaxation properties of the butadiene phase

Sample code	T_{max} (K)	E_a (kJ/mol)	$\epsilon_0 - \epsilon_\infty$	μ_{eff} (X 10^{31} Cm)	ϵ' (298K)
PB	191.7	110	0.092	5.8	2.09
30 SP	191.4	116	0.072	6.0	2.22
30 SD 2.5	192.1	104	0.071	5.9	2.20
30 SD 3.8	191.2	107	0.071	5.7	2.24
50 SP	197.5	119	0.046	5.5	2.30
50 SD 2.5	197.9	111	0.042	5.2	2.20
PS	–	–	–	–	2.52
SBS	194	105	–	–	–
SBS	191	–	–	–	–
PB	–	108	–	–	–

rationalized by application of the Simha–Boyer model of the glass transition:

$$(\alpha_r - \alpha_g)T_g = 0.113 \qquad (11)$$

where the suffixes r and g refer respectively to the rubbery and glassy states[50,51]. A decrease in $(\alpha_r - \alpha_g)$ leads to an increase in T_g and hence in T_{max}. Above $v_{ps} = 0.6$ the samples have a continuous polystyrene phase and the value of $(\alpha_r - \alpha_g)$ and T_{max} remain virtually independent of any further increase in the volume fraction of polystyrene.

The relaxation magnitude at T_{max}, obtained by graphical integration of the area under the $\epsilon'' - 1/T$ curve, is a linear function of the volume fraction of polybutadiene, indicating that any mixing of styrene and butadiene segments at the phase boundaries is not detectable. Analysis of the relaxation magnitude is made using the Kirkwood relation[52]:

$$\frac{(\epsilon_0 - \epsilon_\infty)(2\epsilon_0 + \epsilon_\infty)}{\epsilon_0(\epsilon_\infty + 2)^2} = \frac{gN\mu^2}{9kT\epsilon} \qquad (12)$$

where N is the number of butadiene monomers per unit volume. Assuming as a first approximation $g = 1$, *Table 3* indicates that the average dipole moment per monomer unit is $5.7 \pm 0.5 \times 10^{-31}$ Cm. Since polybutadiene contains 50% of the dielectrically inactive *trans* isomer[59,60], the effective dipole moment of the *cis* (40%) and vinyl (10%) isomers is 8.2×10^{-31} Cm and can be compared with the dipole moments observed in small molecules with similar structures[61], (cyclobutene)–(cyclohexane) $\times 10^{-31}$ Cm.

It is of interest to note that the inclusion of benzoic acid in the sample has no effect on the dipole orientation relaxation of the polybutadiene. A previous study[47] of the relaxation in an SBS copolymer containing 77 vol % polybutadiene exhibited similar relaxation behaviour and identical microstructure to that reported here. The magnitude of the loss amplitude was, however, significantly greater than observed in these studies and the loss factor increased steeply above 330K. Our studies of plasticized SBS exhibited similar behaviour.

Low frequency dielectric behaviour

D.c. transient experiments. The current–time plot obtained after step removal of voltage from the copolymer with 50 wt % polystyrene (*Figure 4*) shows a monotonic decrease with increasing time. The decay current for the copolymer with 30 wt % polystyrene undergoes a slight change in slope, moving to shorter times as the temperature is increased, and is just resolved at 354K as a step in the curve. This type of behaviour is expected if a thermally-activated relaxation is superimposed on a discharge process described by an activated t^{-n} law.

In order to magnify the low frequency electrical properties, benzoic acid dopant, expected to enhance preferentially the conductivity of one phase or of the interphase boundary region was added to the sample. As a result a well-defined relaxation step in the decay was observed. Resolution of the decay current into two components by graphical extrapolation of the long time decay followed by Fourier transformation enables the permittivity–frequency data in *Figure (5)* to be obtained. Apparent activation energies (*Table 4*) were obtained from the linear portions of the Arrhenius plots of relaxation frequency in *Figure 6*.

D.c. conductivities and absorption currents. The conductivities of the samples increased with butadiene content and

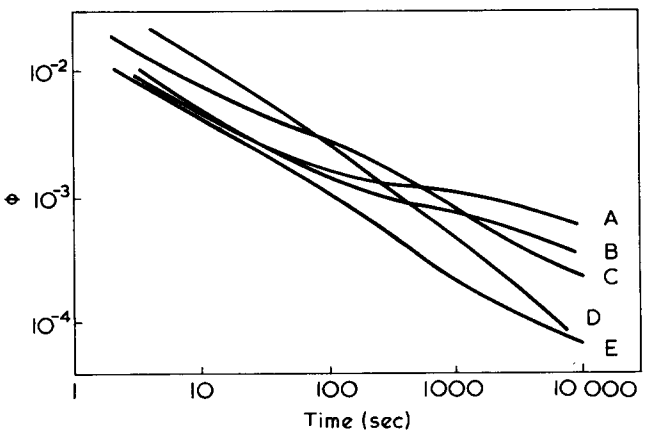

Figure 4 Normalized discharge traces, A. 30 SD 2.5 (351.3K); B, 30 SD 3.8 (350.7K); C, 30 SP (351.5K); D, 50 SP (353.7K); E, 50 SD 2.5 (353.3K)

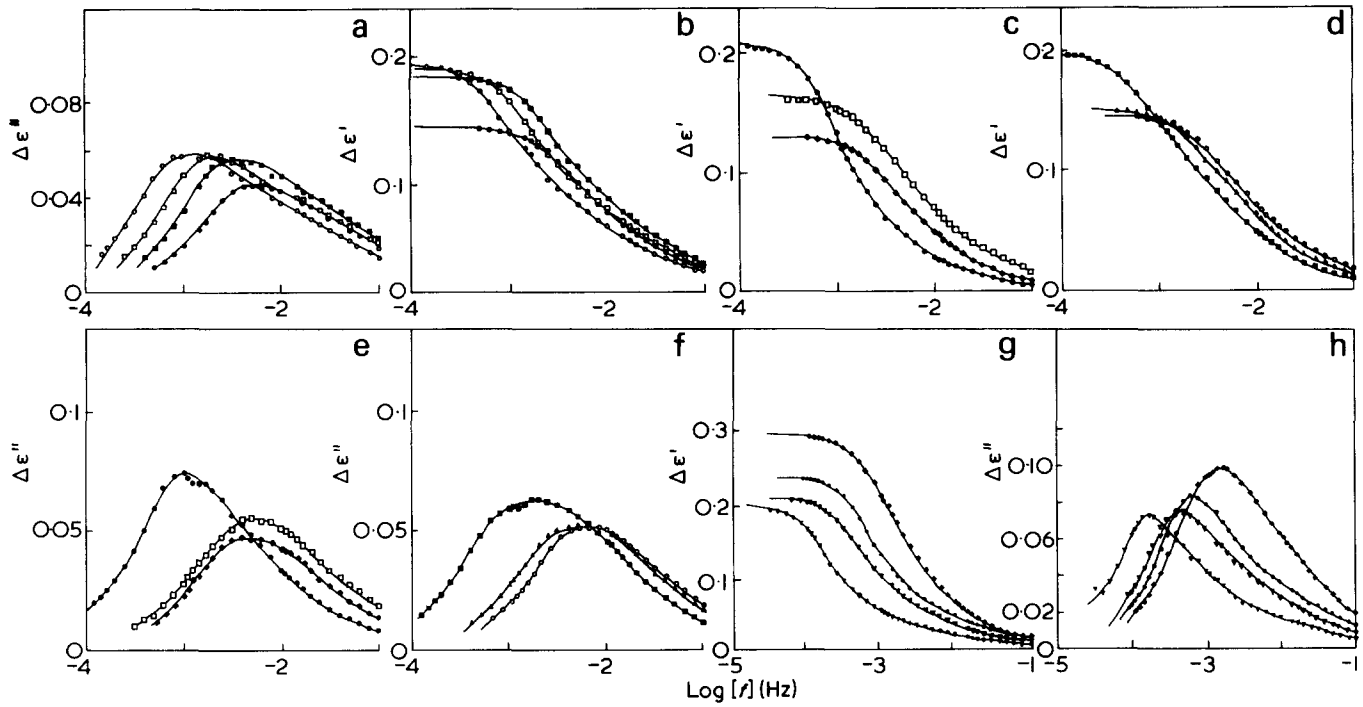

Figure 5 Resolved low frequency relaxation in 30 SD 2.5 [(a) and (b)] and in 30 SD 3.8 [(c)–(f)]. 30 SD 2.5; ○, 333.8K; □, 344.8K; ■, 351.3K ◆, 361.0K; 30 SD 3.8; ●, 332.0K; ■, 342.4K; ◆, 350.8K; ▲, 357.9K; ○, 364.4K; □, 368.3K. Resolved low-frequency relaxation in 50 SD 2.5 [(g) and (h)] ▼, 335.5K; ▽, 346.1K; ○, 353.3K; ◆, 362.5K. Symbol code, *Table 2*

Table 4 Apparent activation energies for d.c. conduction and relaxation

	Activation energy (kJ/mol)	
Sample code	D.c. conductivity	Relaxation
30 SP	65	–
30 SD 2.5	55	56
30 SD 3.8	71	68
30 SP	88	–
50 SD 2.5	84	82

lie below that of pure polybutadiene, $5 \times 10^{-17}\ \Omega^{-1}\,m^{-1}$ at 322K. The conductivity of polystyrene is typically $10^{-21}\ \Omega^{-1}\,m^{-1}$ and there is evidence that its origin lies in long time dipolar reorientation losses rather than in charge transport. These data indicate that the polybutadiene is the more conducting phase in SBS copolymers. The increase in activation energy with increasing styrene content reflects the change from a continuous polybutadiene morphology to one in which both phases are semicontinuous. This explanation is also consistent with a conduction mechanism in which charge transport occurs at least partly in the interface between the styrene and butadiene phases. The increased d.c. conductivity upon addition of benzoic acid may be attributed to either an increase in the number of charge carriers or to mobility associated with masking of the trapping sites. It is interesting to note that the long time absorption currents which are probably due to charge transport and trapping in the more conducting regions are reduced on addition of benzoic acid.

The 100 sec isochronal decay function ϕ_{100} (resolved by subtracting the current extrapolated from long times from the observed current) in the doped copolymer samples also shows a decrease at temperatures above the glass transition temperature of the polystyrene domains (*Figure 7*). This behaviour is consistent with a decrease in the local concen-

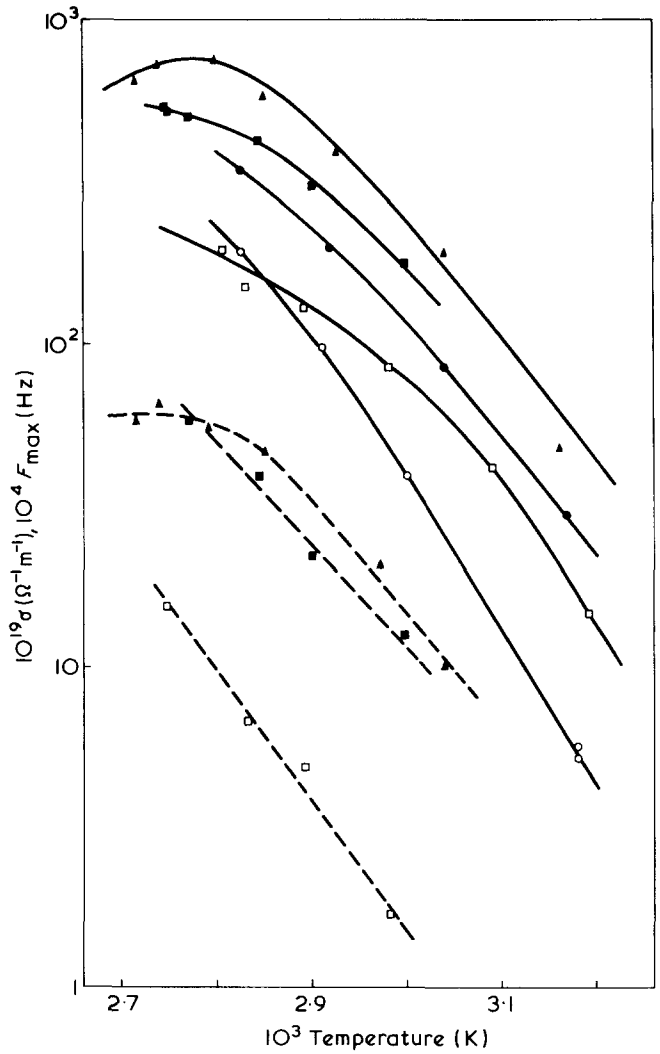

Figure 6 Arrhenius plots. (———), D.c. conductivity; (– – – –), relaxation frequencies: ●, 30 SP; ■, 30 SD 2.5; ▲, 30 SD 3.8; ○, 50 SP; □ 50 SD 2.5. Symbol code, *Table 2*

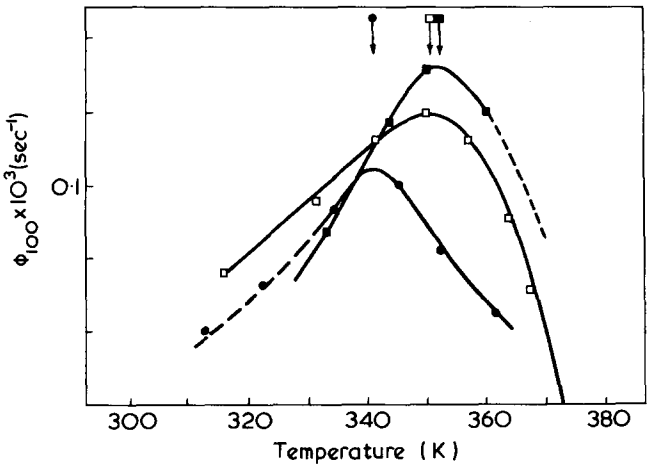

Figure 7 Temperature dependence of the Hamon transformed 100 sec isochronal absorption (subtraction) current I_{100}. ■, 30 SD 2.5; □, 30 SD 3.8; ●, 50 SD 2.5. Glass transitions temperature are indicated by the appropriately designated arrows

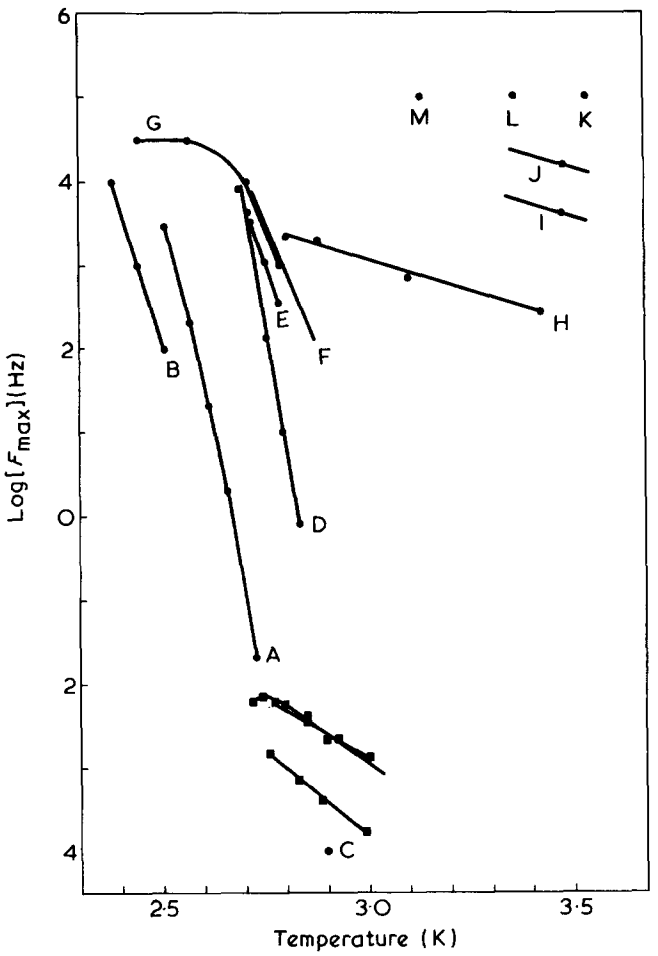

Figure 8 Comparison of the frequency–temperature loci of dipole relaxations with the low frequency processes in SBS. ■, Present data; A, B, C-PS α-process[53–55]. Dopant molecular relaxations coupled to PS α-motions. D, tetracyclone[56]; E, anthrone[56]; F, cholest-4-en-3-one[56]; G, Imidazoline sufactant[37], Dopant molecule relaxations coupled to PS–β motions; H, thianthrene[57]; I, cyclohexyl bromide[57]; J, cyclohexyl chloride[57]; SBR α-process; K, 3 0 wt % styrene[58]; L, 50 wt % styrene[58]; M, 58 wt % styrene[58]

tration of the charge carriers in the polybutadiene regions as solubility in polystyrene occurs above the T_g of the polystyrene phase. It should be noted that the T_g of the 2.5% doped 50 wt % polystyrene sample is lower than that of the pure copolymer.

Resolved low frequency relaxation process. The low frequency relaxation process may be due to either dipole orientation or limited charge carrier migration. Dipole relaxation may occur by molecular motion of the polystyrene domains or in the interfacial region. Dopant molecules residing in these regions can also contribute a relaxation process by motions which may be closely coupled to or independent of the polymer matrix. However these dipole mechanisms can be eliminated by comparison of expected frequency–temperature loci with those observed in this study (*Figure 8*) and by evaluation of the relaxation magnitude which is larger than could be expected for the dipole process described previously[53–57]. Instead, the similarity in the activation energies for d c. conduction and the relaxation process indicate a charge transport mechanism. A model of localized charge carrier hopping in the polybutadiene phase would predict that the relaxation magnitude should decrease and the relaxation time remain constant as the volume fraction of polystyrene, v_{ps}, increases. This is not in agreement with the experimental data. The dependences of both relative magnitude and time on v_{ps} are in accord with an interfacial polarization involving charge trapping at the phase boundaries.

The relaxation magnitude in the 30 wt % copolymer decreases about the T_g whereas that of the 50 wt % polystyrene polymer increases above T_g (*Figure 9*). It may be postulated that, on passing through the T_g of the polystyrene domain the effective volume impermeable to charge carriers (equivalent to v), decreases. Inspection of the MWS equation for a system of long thin rods, $A_a = 0\, A_b = A_c \rightarrow 0.5$ with $\sigma_1 \gg \sigma_2$ reveals that $\Delta\epsilon$ decreases with v_2. So the model

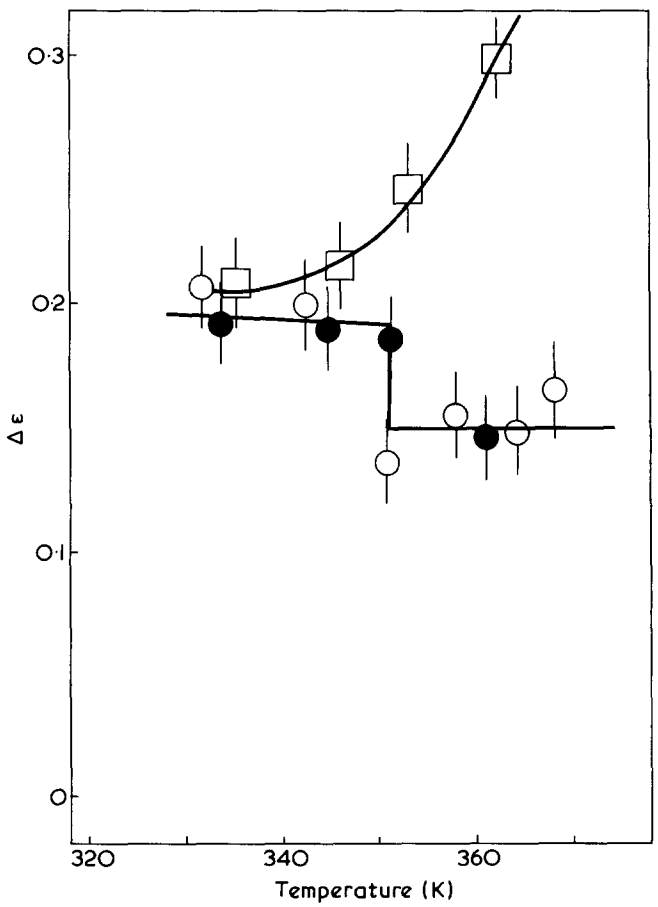

Figure 9 Temperature dependence of the relaxation magnitude ●, 30 SD 2.5; ○, 30 SD 3.8; □, 50 SD 2.5. Symbol code, *Table 2*

Table 5 Calculation MWS relaxation parameters. Constants: polybutadiene $\epsilon_1 = 1.95$; $\sigma_1 = 7 \times 10^{-17}\ \Omega^{-1}\ m^{-1}$ $v_2 = 0.2$; polystyrene $\epsilon_2 = 2.5$; $\sigma_2 = 0$

Morphology	ϵ_∞	$\Delta\epsilon$	(s)	10^{-17} $\Omega^{-1}\ m^{-1}$
(A) 30 SD 2.5 at 351.3K				
(a)	2.11	0.006	24.7	4.90
(b)	2.10	0.723	41.6	3.87
(c)	2.10	0.483	41.6	4.29
Experimental	2.09	0.148	40.8	4.18
(B) 50 SD 2.5 at 353.3K				
(a)	2.20	0.00	–	3.78
(b)	2.17	3.264	61.8	2.2×10^{-3}
(c)	2.19	1.008	a = 61.8 b = 28.4	2.52
Experimental	2.09	0.246	234.0	1 45

predicts that the relaxation magnitude in the copolymer 30 wt % polystyrene will remain constant up to T_g, whereupon it should evidence a decrease. For a lamellar morphology, $A_a = 1$ $A_b = A_c = 0$, with $\sigma_1 \gg \sigma_2$, the relaxation magnitude increases as v_2 decreases, in agreement with the observed behaviour.

Comparison of theory and experiment

30 wt % polystyrene copolymers. These copolymers consist of long cylinders of polystyrene dispersed in a butadiene matrix. Three geometries are amenable to calculation using the simple MWS theory: (a) long axis (a) of cylinders parallel to the electric field[9]; (b) long axis of cylinders perpendicular to the electric field[9]; (c) randomly oriented cylinders or grains[18].

Calculations for cylinders 20 nm in diameter and 1.2 μm long ($a/b = 60$, $A_a = 10^{-3}$, $A_b = A_c = 0.4995$) (*Table 5a*) indicate that the relaxation magnitude is severely underestimated by morphology (a), while there is good agreement with morphologies (b) and (c). Although this simple theory is known to be deficient for the volume fractions of occluded phase obtaining in these polymers, there is no precise treatment for concentrated non-spherical systems.

The observed relaxation time and bulk d.c. conductivity are in excellent agreement with those calculated for morphology (c) with an extrapolated value of the polybutadiene conductivity of $\sigma_1 = 7 \times 10^{-7}\ \Omega^{-1}m^{-1}$, at 333.2K $\sigma_1 = 5 \times 10^{-7}\ \Omega^{-1}\ m^{-1}$.

The use of a different conductivity for polybutadiene leads to significantly poorer agreement for τ and σ without affecting $\Delta\epsilon$, while alteration of the rod dimension ($A_a = 10^{-2}$–10^{-4}) does not alter the calculated relaxation parameters.

The fit of theory to experiment is considerably better than has been obtained in previous studies[29–32] of interfacial polarization in polymers.

The success of the relatively unsophisticated theory without any necessity of introducing surface conductivity or a finite interdomain boundary region must reflect the high degree of order or regularity in the two-phase structure, and the general non-polarity of the phases.

The observed low frequency relaxation shows an asymmetric distribution of relaxation times. Although a distribution of domain sizes exists, theory predicts that the relaxation time distribution is insensitive to variation of the phase dimensions. A more probable source of the skewed distribution would be the combination of parallel and perpendicular cylinder orientations.

50 wt % polystyrene copolymers. These copolymers exhibit an alternating lamellar morphology and may be treated using the expressions for ellipsoidal arrays with $A_a = 1$ and $A_b = A_c = 0$. As before three geometries may be assumed: (1) long axis (b) of lamellae parallel to the electric field[9]; (2) long axis (b) of lamellae perpendicular to the electric field[9]; (3) randomly oriented lamellae or grains[18].

Calculations for the perpendicular morphology seriously underestimate the d.c. conductivity (*Table 5b*). It may be concluded that Maxwell's layered dielectric structure is not applicable in this case. Rather, the observed d.c. conductivity suggests that the sample is semicontinuous in polybutadiene. Morphologies (1) and (3) give rise to continuous or semicontinuous polybutadiene phases and result in d.c. conductivities and relaxation times which are in reasonable agreement with experiment. Moreover since morphology (a) does not lead to a permittivity increment, calculations based on a random or partly random–partly parallel morphology best describe the experimental results. This is in agreement with the electron microscopy observations.

Again the simple MWS theory, with approximate allowance for high volume fraction effects, is adequate for explanation of all the experimental observations although underestimating the relaxation time somewhat. No necessity to introduce complex phenomena associated with charge migration in a diffuse boundary layer is apparent. This is in contrast to the situation in polar phase-separated copolymers, as will be detailed in a later paper. To a large extent this must be due to the relative molecular uniformity of these three block systems, and to the degree of perfection and long range order in the phase separation.

For the volume fractions of constituent phases represented by the 30% and 50% SBS copolymers, modification of the equations for the effects of interdomain interaction in the case of rod or lamellar like morphologies[10,20] is unnecessary and does not lead to a better prediction of relaxation behaviour.

CONCLUSIONS

The high frequency (kHz) dielectric relaxation spectrum shows a single loss peak due to the α relaxation in the polybutadiene phase. The relaxation parameters are dependent on the volume constraints placed on the polybutadiene by the polystyrene phase.

The relaxation due to interfacial polarization was found to be in good agreement with the predictions of MWS theory corrected for effects due to high volume fraction of the polystyrene phase.

No evidence was found for a dielectric effect requiring the existence of a diffuse interface between the styrene–butadiene domains.

The bulk d.c. conductivity was also found to be controlled by the morphology, and also correlated with predictions using the same parameters as those involved in calculation of the relaxation effects.

The temperature dependence of the relaxation magnitude for both of the SBS copolymers was consistent with a decrease in the volume fraction impermeable to charge carriers above the glass transition temperature of the polystyrene phase. Charge trapping in the softened regions of the styrene do-

mains also accounts for the observed decrease in $d\log\sigma/d(1/T)$ and the variation of the long time component of the discharge current above T_g.

ACKNOWLEDGEMENTS

One of us (A.D.W.) would like to thank the SRC for a Research Studentship. The authors would also like to thank Dr C. Price and Miss R. A. Stubbersfield (University of Manchester) for the electron micrographs. The authors also wish to acknowledge the support of the SRC in providing equipment for the Polymer Research at the University of Strathclyde.

REFERENCES

1 Ward, I. M. 'The Mechanical Properties of Polymers',
2 Truell, R., Elbaum, C. and Chick, B. B. 'Ultrasonic Methods in Solid State Physics', Academic Press, New York, 1969
3 Barrer, R. M. in 'Diffusion in Polymers' (Eds J. S. Crank and G. S. Park) Academic Press, London, 1968
4 Peterlin, A. *J. Macromol. Sci. (B)* 1975, **11**, 57
5 Baird, M. E. 'Electrical Properties of Polymeric Materials', The Plastics Institute, London, 1973
6 Ishida, Y. *J. Polym. Sci. (A-2)* 1969, **30**, 1019
7 Van Beek, L. K. H. *Prog. Dielectr.* 1967, **7**, 69
8 Jux, J. T., North, A. M. and Kay, R. M. *Polymer* 1974, **15**, 799
9 Sillars R. W. *J. Inst. Electr. Eng.* 19 , **80**, 378
10 Wagner, K. W. *Arch. Elecktrotech* 1914, **2**, 378
11 Davies, W. E. A. *J. Phys. (D)* 1974, **7**, 120
12 Bruggeman, D. A. G. *Ann. Phys. (Leipzig)* 1935, **24**, 636
13 Looyenga, H. *Physica* 1975, **31**, 401
14 Davies, W. E. A. *J. Phys. (D)* 1974, **7**, 1016
15 McDonald, J. R. *J. Chem. Phys.* 1971, **54**, 2026
16 Adamec, V. *J. Polym. Sci. (A-2)* 1968, **6**, 1241
17 Wyllie, G. in 'Dielectric and Related Molecular Processes', (Ed. M. Davies) Chemical Society, London
18 Fricke, H. *J. Phys. Chem.* 1953, **57**, 934
19 Hanai, T. *Kolloid Z.* 1960, **171**, 23
20 Hanai, T. in 'Emulsion Science' (Ed. P. Sherman) Academic Press, London, 1968
21 Van Beck, L. K. H., Booy, J. and Looyenga, H. *Appl. Sci. Res.* 1965, **12**, 57
22 Mandel, M. *Physica* 1961, **27**, 827
23 Trukhan, E. M. *Sov. Phys. Solid State* 1963, **4**, 2560
24 Dukhin, S. S. and Shilov, V. N. 'Dielectric Phenomena and the Double Layer in Disperse Systems and Polyelectrolytes', Wiley, New York, 1974
25 Pauly, H. and Schwan, H. P. *Z. Naturforsch. (B)* 1959, **14**, 125
26 O'Konski, C. T. *J. Phys. Chem.* 1960, **64**, 605
27 Schwarz, G. *J. Phys. Chem.* 1962, **66**, 2636
28 Takashima, S. *Adv. Chem. Ser.* 1967, **63**, 232
29 Hiroto, S., Saito, S. and Nakajima, J. *Kolloid Z. Z. Polym.* 1966, **213**, 109
30 Hirota, S., Saito, S. and Nakajima, T. *Rep. Prog. Polym. Phys. Jpn* 1967, **10**, 425
31 Baird, M., Goldsworthy, G. T. and Creasy, C. J. *Polymer* 1971, **12**, 159
32 North, A. M. and Reid, J. C. *Eur. Polym. J.* 1972, **8**, 1129
33 Michel, R., Seytre, G. and Maitrot, M. *J, Polym. Sci. (Polym. Phys. Edn)* 1975, **13**, 1333
34 Dev, S. B., North, A. M. and Reid, J. C. in 'Dielectric Properties of Polymers' (Ed. F. E. Karasz) Plenum Press, New York, 1972, p 217
35 Reid, J. C. *Thesis* University of Strathclyde (1972)
36 Keith, H. D. *Kolloid Z. Z. Polym.* 1969, **231**, 421
37 Kosaki, M. and Ieda, M. *J. Phys. Soc. Jpn* 1969, **27**, 1604
38 Yano, S., Tadano, K., Aoki, K. and Koizumi, N. *J. Polym. Sci. (Polym. Phys. Edn)* 1974, **12**, 1875
39 Scheiber, D. J. *J. Res. Nat. Bur. Stand (C)* 1961, **65**, 23
40 Reddish, W. *J. Polym. Sci. (C)* 1966, **14**, 123
41 Dev, S. B., North, A. M. and Pethrick, R. A. *Adv. Mol. Relaxation Processes* 1972, **4**, 159
42 Kato, K. *Polym. Eng. Sci.* 1967, **7**, 38
43 Folkes, M. J. and Keller, A. in 'The Physics of Glassy Polymers' (Ed. R. N. Haward) Applied Science, London 1973
44 Lewis, P. R. and Price, C. *Polymer* 1972, **13**, 20
45 Kampf, G., Kromer, H. and Hoffman, M. *J. Macromol. Sci. (B)* 1972, **6**, 167
46 Meier, D. J. *Polym. Prepr.* 1974, **15**, 171
47 Shen, M., Kaniskin, V. A., Biliyar, K. and Boyd, R. H. *J. Polym. Sci. (Polym. Phys. Edn)* 1973, **11**, 2261
48 Maekawa, E., Maneke, R. G. and Ferry, J. D. *J. Phys. Chem.* 1965, **69**, 2811
49 Hendus, H., Illers, K. H. and Ropte, E. *Kolloid Z. Z. Polym.* 1967, **216-7**, 110
50 Anderson, J. E. and Liu, K. J *Macromolecules* 1971, **4**, 260
51 Boyer, R. F. *J. Polym. Sci. (Polym. Symp.)* 1975, **50**, 189
52 Onsager, L. *J. Am. Chem. Soc.* 1936, **58**, 1486
53 Adamec, V. *Kolloid Z. Z. Polym.* 1969, **237**, 219
54 Saito, S. and Nakajma, T. *J. Appl. Polym. Sci.* 1959, **11**, 93
55 Sawa, G., Ito, O., Morita, S. and Ieda, M. *J, Polym. Sci. (Polym. Phys. Edn)* 1974, **12**, 1231
56 Davies, M. and Edwards, A. *Trans. Faraday Soc.* 1967, **63**, 2163
57 Davies, M. and Swain, J. *Trans. Faraday Soc.* 1971, **67**, 1637
58 Fujimoto, K. and Yoshimura, N. *Rubber Chem. Technol.* 1968, **41**, 1109
59 Santree, E. R., Chang, R. and Morton, M. *J. Polym. Sci. (Polym. Lett)* 1973, **11**, 449
60 Spectra, E. R., Mochel, V. C. and Morton, M. *J. Polym. Sci. (Polym. Lett.)* 1973, **11**, 453
61 Chen, C. Y., Le Fevre, R. J., Sundaram, K. N. S. *J, Chem. Soc.* 1965, p 553